Letters

1.37 kV/12 A NiO/β-Ga_2O_3 Heterojunction Diode With Nanosecond Reverse Recovery and Rugged Surge-Current Capability

Hehe Gong, *Student Member, IEEE*, Feng Zhou, Weizong Xu, Xinxin Yu, Yang Xu, Yi Yang, Fang-fang Ren, Shulin Gu, Youdou Zheng, Rong Zhang, Hai Lu, *Senior Member, IEEE*, and Jiandong Ye, *Member, IEEE*

***Abstract*—Ga_2O_3 power diodes with high voltage/current ratings, superior dynamic performance, robust reliability, and potentially easy-to-implement are a vital milestone on the Ga_2O_3 power electronics roadmap. In this letter, a better tradeoff between fast reverse-recovery and rugged surge-current capability has been demonstrated in NiO/Ga_2O_3 p-n heterojunction diodes (HJDs). With the double-layered p-NiO design, the HJD exhibits superior electrostatic performances, including a high breakdown voltage of 1.37 kV, a forward current of 12.0 A with a low on-state resistance of 0.26 Ω, yielding a static Baliga's figure of merit (FOM) of 0.72 GW/cm^2. Meanwhile, the fast switching performance has been observed with a short reverse recovery time in nanosecond timescale (11 ns) under extreme switching conditions of d*i*/d*t* up to 500 A/μs. In particular, for a 9-mm^2 HJD, a large surge current of 45 A has also been obtained in a 10-ms surge transient, thanks to the conductivity modulation effect. These results are comparable with those of the advanced commercial SiC SBDs and have significantly outperformed the past reported Ga_2O_3 HJDs, fulfilling the enormous potential of Ga_2O_3 in power applications.**

***Index Terms*—Fast reverse recovery, Gallium oxide (Ga_2O_3), NiO, p-n heterojunction diode (HJD), surge current..**

I. Introduction

GALLIUM oxide (Ga_2O_3) materials have invoked great interest for power devices applications. The attractive properties of β-Ga_2O_3, such as an ultrawide bandgap of ~4.8 eV and high breakdown electric field exceeding 8 MV/cm, boast β-Ga_2O_3 as a potential replacement of silicon for high-voltage device technologies [1]–[3]. For such superior materials, the unipolar- and bipolar-power devices based on β-Ga_2O_3 are both highly desired for attractive high-power applications in electronic circuits [4], [5]. However, the absence of p-type Ga_2O_3 directly hinders the rational design of bipolar devices [6]. Alternatively, bipolar Ga_2O_3 diodes were realized by using a natively p-type oxide to produce p-n heterojunction diodes (HJDs) involving n-type Ga_2O_3 [7]. Based on this advanced technology, the NiO/Ga_2O_3 HJDs with excellent reverse blocking capability have been recently demonstrated, obtaining a high breakdown voltage (BV) of 1.86 kV [8] and an ultra-low reverse leakage current of below 1 μA/cm^2 [9]. But, a surprising result is that the forward *I–V* characteristics of the reported p-n HJDs are similar to those of unipolar Schottky barrier diode (SBD), presenting linear current conduction instead of bipolar behavior [8], [9]. As being demonstrated in SiC and GaN power diodes, with the bipolar conduction (or the conductivity modulation) from minority carrier injection, the devices not only have advantages in increasing the current density but also can reduce the on-state resistance, leading to a strong surge-current tolerance [10], [11]. Therefore, it is of great importance to identify whether the Ga_2O_3 p-n HJDs are capable of conductivity modulation in the forward bias region, especially during high surge-current operation. The injection and storage of holes in the drift layer may also significantly degrade the dynamic switching performance, due to the minority carrier's recombination/ extraction [12]. Thus, dynamic switching and surge-current performance in Ga_2O_3 HJDs worth specific investigations.

In this letter, with the construction of double-layered p-NiO with β-Ga_2O_3, the large-area (1-mm^2) vertical NiO/Ga_2O_3 HJD exhibits a high BV of 1.37 kV, a forward current of 12.0 A, low on-state resistance of 0.26 Ω, yielding a static Baliga's figure of merit (FOM) of 0.72 GW/cm^2. Furthermore, the 9-mm^2 HJDs deliver a record-high current of 70 A (10-ms surge current of 45 A) and a low on-state resistance (R_{on}) of 65 mΩ, with simultaneously a *BV* of 462 V. Both devices clearly demonstrate the forward conductivity modulation characteristics and inherent reverse blocking capability of the p-n junction. In particular, by implementing these diodes into the board-level inductive switching circuits, ultra-fast switching performance has been observed, presenting a short reverse recovery time of 11 ns with low switching FOM) of 0.85 Ω·nC. This letter, thus, clearly

Manuscript received April 14, 2021; revised May 9, 2021; accepted May 18, 2021. Date of publication May 21, 2021; date of current version July 30, 2021. This work was supported in part by the National Key R&D Program under Grant 2018YFB0406502, in part by the State Key R&D project of Jiangsu under Grants BE2018115 and BE2019103, in part by the State Key R&D project of Guangdong under Grant 2020B010174002, in part by the National Nature Science Foundation under Grant 61774081, and in part by Joint Youth Fund of Ministry of Education for Equipment Pre-Research under Grant 6141A02033237. *(Hehe Gong and Feng Zhou contributed equally to this work.) (Corresponding authors: Hai Lu; Jiandong Ye.)*

The authors are with the School of Electronic Science and Engineering, Collaborative Innovation Center of Advanced Microstructures, Nanjing University, Nanjing 210023, China (e-mail: hhgong@smail.nju.edu.cn; dg1923060@smail.nju.edu.cn; wz.xu@nju.edu.cn; yuxx711@126.com; 1615475524@qq.com; malab@nju.edu.cn; ffren@nju.edu.cn; slgu@nju.edu.cn; ydzheng@nju.edu.cn; rzhang@nju.edu.cn; hailu@nju.edu.cn; yejd@nju.edu.cn).

Color versions of one or more figures in this article are available at https://doi.org/10.1109/TPEL.2021.3082640.

Digital Object Identifier 10.1109/TPEL.2021.3082640

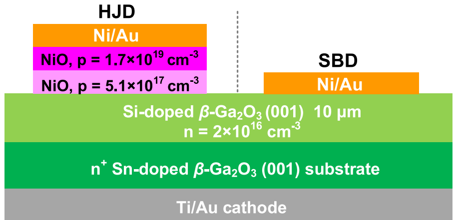

Fig. 1. (a) Schematics cross-section of vertical NiO/β-Ga_2O_3 HJD (left) and Ni/β-Ga_2O_3 SBD (right).

demonstrates the notable potentials of the NiO/Ga_2O_3 HJDs in high-power and high-speed switching applications.

II. Device Fundamentals

Fig. 1 shows the schematic cross-section view of the double-layered NiO/β-Ga_2O_3 p-n HJD on highly conductive Sn-doped (001) β-Ga_2O_3 substrate by hydride vapor phase epitaxy, which consists of 10-μm Si-doped β-Ga_2O_3 drift layer with an electron concentration of 2×10^{16} cm^{-3}, determined by Hall measurement at room temperature. The device process begins with the formation of back-side ohmic contact (cathode) of Ti/Au (20/80 nm) deposited by electron beam evaporation, followed by rapid thermal annealing at 500 °C for 1 min under the N_2 ambient. Subsequently, double-layered p-NiO films are deposited on the drift layer by the radio frequency (RF) magnetron sputtering technique. The RF power is 150 W, and the target is high purity (99.99%) NiO ceramics. More detailed descriptions of the double-layered NiO deposition have been given in our previous work [8]. The Hall measurement characterizations of the double-layered p-NiO films indicate that the 300-nm-thick bottom-side layer and a 100-nm-thick upper-side layer have hole concentrations and mobility of 5.1×10^{17} cm^{-3}, 0.94 cm^2/V·s and 1.7×10^{19} cm^{-3}, 0.3 cm^2/V·s, respectively. Finally, a Ni/Au (300/300 nm) metal stack is deposited on the upper p-NiO layer to form the ohmic contact (anode). Meanwhile, the Ni/β-Ga_2O_3 SBD is also fabricated on the same wafer by identical processes except for the p-NiO deposition underneath the Schottky anode metal.

III. Results and Discussion

A. Static Characteristics

The 1-mm^2 devices encapsulated in TO-220 package are measured using a B1505 power device analyzer in the dc mode. As shown in Fig. 2(a), both the HJD and SBD exhibit a high on/off current ratio of 10^8 with a low subthreshold slop (SS) of $\sim$68 mV/dec, which are comparable with the state-of-art β-Ga_2O_3 SBDs with the implanted edge termination [13]. Meanwhile, the HJD exhibits a turn-ON voltage (V_{on}) of 1.73 V, which is lower than the built-in potential (V_{bi}) of 2.4 V for p-n heterojunction determined from the intercept of 1/C^2-V plot on the *x*-axis [see Fig. 2(b)]. This phenomenon is also observed in Ni/β-Ga_2O_3 SBD with a lower V_{on} of 0.8 V but a higher V_{bi} of 1.2 V. It can be understood that electrons from the conduction band of β-Ga_2O_3 are transferred into valance band of NiO or energy level of Ni mediated by defective states at the large-area interface [14]. The low V_{on} is, therefore, available to Ga_2O_3-based HJDs, which is smaller than GaN p-n diodes with a V_{on} of $\sim$3 V [11], thus remarkably reducing the conduction losses.

To evaluate the current capability of the 1-mm^2 HJD and SBD, the pulsed *I–V* measurements are carried out with a pulse width of 50 μs and a duty cycle of 1% [see Fig. 2(c)] [1], where a high current rectifying level up to 12 A is obtained in both devices. Apparently, the HJD exhibits a continuous reduction of differential R_{on} from >20 to 0.26 Ω with increased forward bias, while R_{on} of the SBD almost keeps a constant value of 0.58 Ω. The significant reduction of R_{on} with a nonlinearity *I–V* characteristic is resulted from the onset of conductivity modulation by the minority carrier injection from the p-type NiO layer, enabling additional electrons accumulated in the drift region and improving the bipolar current spreading in vertical structures. It is noted that the *I–V* characteristics of HJD are also different from the typical silicon-based bipolar diodes, which may be originated that, the bipolar conduction mode in the NiO/Ga_2O_3 HJD is incipiently activated with the limited minority carrier injection at room temperature due to the larger valence band offset at NiO/Ga_2O_3 interface and the relatively low hole mobility in NiO. In unipolar rectifiers, it has been reported that the decreased electron mobility induced by thermally enhanced phonon scattering could lead to severe R_{on} degradation at high temperatures. On the contrary, R_{on} of the bipolar device (such as GaN p-n diodes) increases much slower or even decreases with elevated temperatures, benefiting from the conductivity modulation effect [11]. Indeed, as shown in Fig. 2(d) and (e), with the temperature (*T*) rising from 25 to 175 °C, the R_{on} of HJD was first reduced from 1.06 to 0.77 Ω and then stabilizes at 0.80 Ω, exhibiting a *T*-independent R_{on} behavior as similar in GaN p-n diodes [11], while that of SBD increases monotonically with a positive temperature coefficient of 2 mΩ/°C. Additionally, the values of V_{on} are reduced with elevated temperatures, which are primarily originated from the bandgap narrowing effect and thermally-enhanced carrier diffusion. Combining the merits of *T*-independent R_{on}, high BV and low V_{on}, the Ga_2O_3 HJDs are highly desirable for high-power and high-temperature applications.

Fig. 2(f) shows the reverse *I–V* characteristics of the HJD and SBD. Compared with the SBD with a BV of 245 V, the HJD exhibits a remarkably reduced leakage current with $>10^6\times$ lower in magnitude at considerable bias and an enhanced BV of 1370 V, yielding a static *Baliga's FOM* (BV^2/R_{on}) of 0.72 GW/cm^2. To our best knowledge, the achieved BFOM value is highest among the reported Ga_2O_3 HJDs [8], [15] and comparable to the state-of-the-art Ga_2O_3 SBDs [1], [3], [16]. The BV vs R_{on} of the large-area HJD is also benchmarked with the commercial 650 and 1200-V SiC SBD (C3D02065E, C4D02120A) [see Fig. 2(g)]. Additionally, a high on/off switching ratio of 10^7 ($\sim$10 A at + 9 V/ $\sim10^{-6}$ A at −900 V) has also demonstrated a reliable rectification capability of Ga_2O_3 HJD.

B. Switching Performance

For the practical high-power switching applications, current levels of Ga_2O_3 diodes need to be as high as possible. To this end, the larger area (9-mm^2) Ga_2O_3 diodes have been fabricated

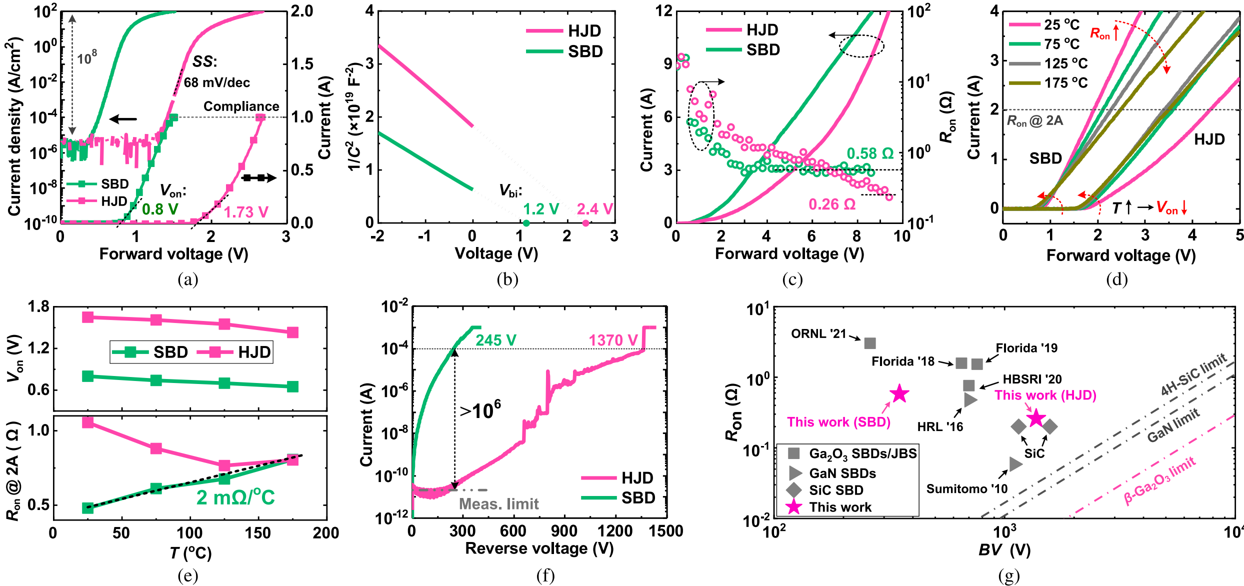

Fig. 2. (a) Forward dc I–V characteristics of the 1-mm^2 HJD and SBD in log scale and linear scale. (b) $1/C^2$ versus voltage measured at 100 kHz. (c) Pulsed I–V characteristics and corresponding R_{on}. (d) T-dependent forward current at temperatures of 25, 75, 125, and 175 °C. (e) T-dependent V_{on} and R_{on}. The R_{on}s are extracted at forward current of 2 A. (f) Reverse I–V characteristics. (g) R_{on} *vs.* BV of this vertical Ga_2O_3 HJD/SBD, benchmarked with the state-of-the-art ~1-mm^2 Ga_2O_3 SBDs/JBS, GaN SBDs, and commercial SiC SBD.

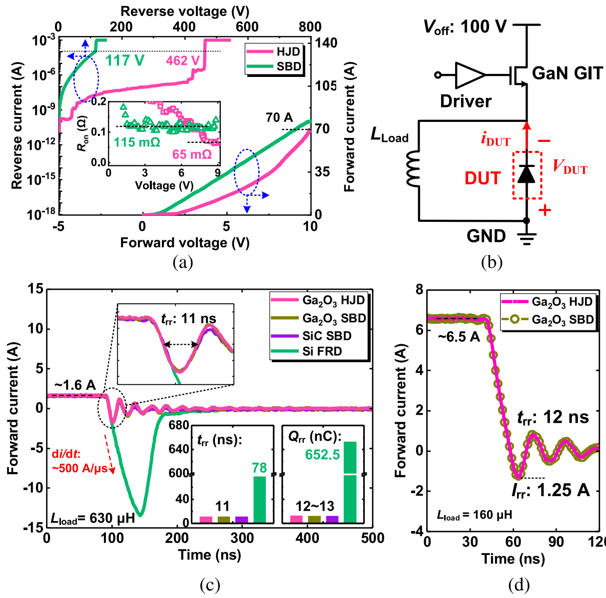

Fig. 3. (a) Reverse I–V characteristics of 9-mm^2 Ga_2O_3 diodes. Inset: The extracted R_{on} from forward I–V measurements. (b) Schematic of the DPT circuit. The fast-speed commercial GaN gate injection transistor has been used as a control switch. (c) Reverse recovery characteristics of different diodes. Inset: Corresponding t_{rr} and Q_{rr}. The t_{rr} is defined as the time when the reverse current recovers to 10% of its peak value, where the Q_{rr} is calculated by the time-integration of reverse current. (d) Reverse recovery waveforms with a high forward current of ~6.5 A.

by extending the area of square anode contacts, which exhibits a highest recorded pulsed current of 70 A among the reported Ga_2O_3 diodes [see Fig. 3(a)]. Moreover, such HJD delivers a BV of 462 V with a low leakage current of 0.1 μA at −400 V, outperforming the SBD with *a BV* of 117 V. Meanwhile, an ultra-low R_{on} of 65 mΩ has been achieved, indicating the highly uniform current distribution within the large-area HJD.

To evaluate the dynamic switching performance of Ga_2O_3-based HJDs, board-level double-pulse-test (DPT) measurements have been performed [17] and the schematic circuit is shown in Fig. 3(b). For a forward conducting rectifier with a high current, a large amount of free carriers are injected into the drift layer. When the device under test (DUT) is switched from on-state to off-state, the stored charges must be fully removed before the build-up of the depletion region to withstand the reverse bias, leading to a reverse recovery process. As shown in Fig. 3(c), under a switching condition from a high forward current (i_{DUT}) of 1.6 A to a reverse bias of 100 V with a fast di/dt of 500 A/μs, the 9-mm^2 HJD exhibits the superior switching performance with a reverse recovery time (t_{rr}) of 11 ns and a reverse recovery charge (Q_{rr}) of 13 nC, which is comparable with that of the commercial SiC SBD and presents apparently lower switching loss than the Si fast-recovery diode (FRD, RF305BM6S). Moreover, the switching FOM ($R_{\mathrm{on}} \times Q_{\mathrm{rr}}$), which is a merit for demonstrating high-speed switching capability, is only 0.85 Ω·nC [17], [18]. Additionally, the small-area 1-mm^2 HJD also exhibits fast switching performance with low reverse recovery losses, when suffering from i_{DUT} of 5 A to a reverse bias of 600 V. These results clearly present the significant potentials of Ga_2O_3 HJD in fast switching operations [19].

By decreasing the load inductor (L_{load}) from 630 to 160 μH in DPT circuit, a higher i_{DUT} of ~6.5 A (almost equal to the rated current i_{rated} ~6.2 A of [3] with the same 9-mm^2 area) is obtained [20], as present in Fig. 3(d). Even when switching from a high forward current, the HJD still shows almost zero-reverse-recovery characteristics with a low t_{rr} of 12.0 ns. It should be noted that Ga_2O_3 HJD and SBD exhibit similar switching behaviors regardless of i_{DUT}. The fast-speed recovery characteristic

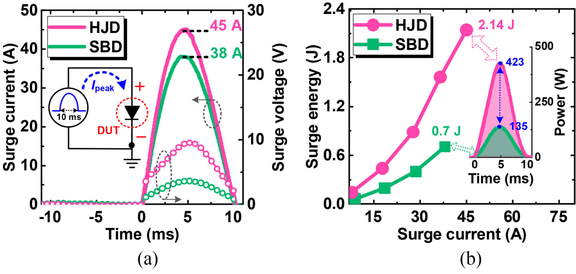

Fig. 4. (a) Surge current and voltage waveforms of the 9-mm^2 HJD and SBD. Inset: The resonance circuit generates a 10-ms half-sine surge current pulse to go through the DUT. (b) Corresponding surge power and energy.

of HJD may be attributed to the short minority-carrier lifetime (τ_{HL}) of p-n diodes at high-level injection. In terms of $\tau_{\mathrm{HL}} = 2\times\ (I_{\mathrm{rr}}/i_{\mathrm{DUT}}) \times t_{\mathrm{rr}}$ [15], the τ_{HL} is determined to be 4.5 ns, which is comparable with the previously reported values [15] and is 70% lower than the t_{rr}. Moreover, the normalized Q_{rr} per device area for the HJD is only 1.3×10^{-7} C/cm^2 during the switching process. The low minority-carrier-stored charge in the drift region is mainly limited by the high barrier height, which could be induced by a large valence band offset of 3.6 eV at NiO/Ga_2O_3 heterojunction [14]. With a short minority carrier lifetime, the stored charges are expected to be rapidly removed during the turn-off process of carrier sweep-out and fast recombination, revealing the intrinsic immunity of Ga_2O_3 HJD to high current switching.

C. Surge Current Ruggedness

With a long-duration high current conducting or at current overshoot/oscillation surging, a huge amount of Joule heat generated within the resistive diodes would lead to an abrupt rise of the junction temperature (T_{j}) [21], [22], which, in turn, cause increased R_{on} and heat accumulation inside the diodes [23], consequently deteriorating the device performance. Therefore, sustaining the low R_{on} under the high current conducting condition is directly meaningful for enhancing the surge current capability. Recently, advanced double-side-cooled package strategies to weaken the temperature dependence of the R_{on} have been demonstrated in 9-mm^2 Ga_2O_3 SBDs [3], successfully boosting the maximum surge current (I_{peak}) from 37.5 to >60 A in a 10-ms duration. By using a similar resonance circuit to generate a half-sinusoidal surge current [3], the 9-mm^2 Ga_2O_3 SBD with standard TO-220 package in this letter can also withstand a comparable I_{peak} of 38 A ($T_{\mathrm{j}} > 600$ K), as present in Fig. 4(a). Moreover, under the identical test conditions, a higher I_{peak} of 45 A is achieved, demonstrating apparently advantageous surge current tolerance of the Ga_2O_3 HJD. Such enhanced surge capability is attributed to the T-independent R_{on} with a rather lower value at a high current level owing to the conductivity modulation effect, whereas the positive temperature coefficient of R_{on} in the SBD results in the severe self-heating effect and, thus, a lower surge current [11]. In particular, with the recorded surge current and voltage waveforms in a 10-ms duration, the corresponding device power and energy dissipation are calculated and summarized in Fig. 4(b). In both diodes, the surge energy is observed to increase with elevated surge current. It is noted that the HJD withstands a higher surge power of 423 W with sustained energy of 2.14 J, which outperforms the SBD counterpart (135 W, 0.7 J). Thus, it is safe to conclude that the Ga_2O_3 HJD is a better candidate for high-reliability power applications.

IV. Conclusion

With the double-layered p-NiO design, large-area 1-mm^2/9-mm^2 NiO/β-Ga_2O_3 p-n HJDs have been demonstrated, yielding a high BV of 1370 V/462 V, a low R_{on} of 260/65 mΩ, and a record-high current of 12 A/70 A, respectively. In particular, ultra-fast switching performance with a reverse recovery time of 11 ns is achieved while maintaining a rugged surge-current tolerance with a surge-current of 45 A. Together with the advantage of high voltage/current ratings, high dynamic performance, high reliability and potentially easy-to-implement, the vertical Ga_2O_3 HJDs present significant potentials in high-power, high-speed, and highly reliable power applications.

References

[1] W. Li, K. Nomoto, Z. Hu, D. Jena, and H. G. Xing, "Field-Plated Ga_2O_3 trench Schottky barrier diodes with a BV^2/$R_{\mathrm{on,sp}}$ of up to 0.95 GW/cm^2," *IEEE Electron Device Lett.*, vol. 41, no. 1, pp. 107–110, Nov. 2019.

[2] M. Ji *et al.*, "Demonstration of large-size vertical ga_2o_3 Schottky barrier diodes," *IEEE Trans. Power Electron.*, vol. 36, no. 1, pp. 41–44, Jun. 2021.

[3] M. Xiao *et al.*, "Packaged ga_2o_3 Schottky rectifiers with over 60 a surge current capability," *IEEE Trans. Power Electron.*, vol. 36, no. 8, pp. 8565–8569, Aug. 2021.

[4] T. Watahiki, Y. Yuda, A. Furukawa, M. Yamamuka, Y. Takiguchi, and S. Miyajima, "Heterojunction p-Cu_2O/n-Ga_2o_3 diode with high breakdown voltage," *Appl. Phys. Lett.*, vol. 111, no. 22, Nov. 2017, Art. no. 222104.

[5] R. Sharma *et al.*, "Effect of probe geometry during measurement of >100 A ga_2o_3 vertical rectifiers," *J. Vac. Sci. Technol. A*, vol. 39, no. 1, Dec. 2021, Art. no. 013406.

[6] S. J. Pearton, F. Ren, M. Tadjer, and J. Kim, "Perspective: Ga_2o_3 for ultra-high power rectifiers and MOSFETS," *J. Appl. Phys.*, vol. 124, no. 22, Dec. 2018, Art. no. 220901.

[7] S. J. Pearton *et al.*, "A review of ga_2o_3 materials, processing, and devices," *Appl. Phys. Rev.*, vol. 5, no. 1, Jan. 2018, Art. no. 011301.

[8] H. H. Gong, X. H. Chen, Y. Xu, F. F. Ren, S. L. Gu, and J. D. Ye, "A 1.86-kV double-layered NiO/β-Ga_2o_3 vertical p–n heterojunction diode," *Appl. Phys. Lett.*, vol. 117, no. 2, Jul. 2020, Art. no. 022104.

[9] X. Lu *et al.*, "1-kV sputtered p-NiO/n-Ga_2O_3 heterojunction diodes with an ultra-low leakage current below 1 μA/cm^2," *IEEE Electron Device Lett.*, vol. 41, no. 3, pp. 449–452, Jan. 2020.

[10] N. Ren, J. Wu, L. Liu, and K. Sheng, "Improving surge current capability of SiC merged PiN schottky diode by adding plasma spreading layers," *IEEE Trans. Power Electron.*, vol. 35, no. 11, pp. 11316–11320, Apr. 2020.

[11] S. W. Han, S. Yang, Y. K. Li, Y. X. Liu, and K. Sheng, "Photon-enhanced conductivity modulation and surge current capability in vertical GaN power rectifiers," in *Proc. IEEE Int. Symp. Power Semicond. Devices IC's*, May 2019, pp. 63–66.

[12] D. L. Mauch *et al.*, "Ultrafast reverse recovery time measurement for wide-bandgap diodes," *IEEE Trans. Power Electron.*, vol. 32, no. 12, pp. 9333–9341, Mar. 2017.

[13] H. Zhou *et al.*, "High-Performance vertical β-Ga_2o_3 Schottky barrier diode with implanted edge termination," *IEEE Electron Device Lett.*, vol. 40, no. 11, pp. 1788–1791, Sep. 2019.

[14] H. Gong *et al.*, "Band alignment and interface recombination in NiO/β-Ga_2o_3 Type-II p-n heterojunctions," *IEEE Trans. Electron Devices*, vol. 67, no. 8, pp. 3341–3347, Jun. 2020.

[15] Y. Hu *et al.*, "1.2 kV/2.9 mΩ·cm^2 vertical NiO/β-Ga_2o_3 Heterojunction diodes with high switching performance," in *Proc. IEEE Int. Symp. Power Semicond. Devices IC's*, Sep. 2020, pp. 178–181.

[16] Y. Lv *et al.*, "Demonstration of β-Ga_2o_3 junction barrier Schottky diodes with a Baliga's figure of merit of 0.85 GW/cm^2 or a 5A/700 v handling capabilities," *IEEE Trans. Power Electron.,* vol. 36, no. 6, pp. 6179–6182, Nov. 2020.

[17] S. Han, S. Yang, R. Li, X. Wu, and K. Sheng, "Current-collapse-free and fast reverse recovery performance in vertical GaN-on-GaN Schottky barrier diode," *IEEE Trans. Power Electron.,* vol. 34, no. 6, pp. 5012–5018, Jun. 2019.

[18] Y. Wei *et al.*, "Experimental study on static and dynamic characteristics of ga_2o_3 Schottky barrier diodes with compound termination," *IEEE Trans. Power Electron.,* p. 1, Mar. 2021.

[19] Q. He *et al.*, "Schottky barrier rectifier based on (100) β-Ga_2o_3 and its DC and AC characteristics," *IEEE Electron Device Lett.,* vol. 39, no. 4, pp. 556–559, Feb. 2018.

[20] R. Mitova, R. Ghosh, U. Mhaskar, D. Klikic, M.-X. Wang, and A. Dentella, "Investigations of 600-V GaN HEMT and GaN diode for power converter applications," *IEEE Trans. Power Electron.,* vol. 29, no. 5, pp. 2441–2452, May 2014.

[21] F. Zhou *et al.*, "Demonstration of avalanche and surge-current robustness in GaN junction barrier schottky diode with 600 V/10 a switching capability," *IEEE Trans. Power Electron.,* p. 1, Apr. 2021.

[22] E. Van Brunt, T. Barbieri, A. Barkley, J. Solovey, J. Richmond, and B. Hull, "Surge current failure mechanisms in 4H-SiC JBS rectifiers," in *Proc. IEEE Int. Symp. Power Semicond. Devices IC's*, May 2018, pp. 415–418.

[23] J. León *et al.*, "Temperature effects on the ruggedness of SiC schottky diodes under surge current," *Microelectron. Rel.,* vol. 54, no. 9/10, pp. 2207–2212, Aug. 2014.